We are IntechOpen,
the world's leading publisher of Open Access books
Built by scientists, for scientists

6,900
Open access books available

186,000
International authors and editors

200M
Downloads

Our authors are among the

154
Countries delivered to

TOP 1%
most cited scientists

12.2%
Contributors from top 500 universities

Selection of our books indexed in the Book Citation Index
in Web of Science™ Core Collection (BKCI)

Interested in publishing with us?
Contact book.department@intechopen.com

Numbers displayed above are based on latest data collected.
For more information visit www.intechopen.com

Coherence Correlation Interferometry in Surface Topography Measurements

Wojciech Kaplonek and Czeslaw Lukianowicz
Koszalin University of Technology
Poland

1. Introduction

Assessment of surface topography can be done by various methods, especially stylus and optical methods as well as utilising scanning tunneling microscopes and atomic force microscopes (Whitehouse, 1994, 2003; Thomas, 1999; Wieczorowski, 2009). The most accurate techniques for assessing surface topography include optical methods (Leach, 2011), especially methods of interference (Pluta, 1993; Hariharan, 2007). In the last two decades, there have been rapid developments in interferometry, as a result of the new possibilities for digital recording and analysis of interference images. The fastest growing interference methods include Phase Stepping Interferometry (PSI) (Creath, 1988; Stahl, 1990; Kujawinska, 1993; Creath & Schmit, 2004) and methods based on coherence analysis of light reflected from the test and reference surfaces (Harasaki et al., 2000; Blunt & Jiang, 2003; Schmit, 2005; Blunt, 2006; Petzing et al., 2010). This second group of methods is defined in different terms in English (Petzing et al., 2010; Leach, 2011), for example:

- Coherence Correlation Interferometry (CCI),
- Coherence Probe Microscopy (CPM),
- Coherence Scanning Microscopy (CSM),
- Coherence Radar (CR),
- Coherence Scanning Interferometry (CSI),
- Coherence Scanning Microscopy (CSM),
- Scanning White Light Interferometry (SWLI),
- Vertical Scanning Interferometry (VSI),
- White Light Scanning Interferometry (WLSI).

Modern methods of interferential microscopy used for the assessment of surface topography are based on automated interference image analysis and coherence analysis (Deck & de Grot, 1994; Patorski et al., 2005; de Grot & Colonna de Lega, 2004; Niehues et al., 2007). Assessment of surface topography requires that all of the information contained in one or more interference images, be porcessed in a sufficiently brief period of time. This process was made possible by:

- progress in the development of photodetectors,
- several hundred-fold increase in computing power,
- technological improvements in effective data storage,

- dynamic development of photonic engineering,
- development of new algorithms for digital interference image processing,
- development of advanced specialized computer software.

PSI methods (Hariharan & Roy, 1995) consist in the analysis of the light phase distribution on the measured surface. They enable the highly accurate measuring of the height of surface irregularities. The measuring range of these methods, however, is relatively small, while methods based on tracking and analysing the degree of temporal coherence of the interfering waves offer the possibility to measure the height irregularities of the surface over a greater range. Some of the measuring instruments used have the capacity to execute both methods. The principles and use of Coherence Correlation Interferometry (CCI) in surface topography measurements are presented in this chapter.

2. General characteristics of CCI

A brief introduction will present the characteristics of interference-based methods used in surface topography measurement, forming a background that highlights the advantages of CCI. The second section will include:

- presentation of the general characteristics of CCI,
- an overview of the general idea of the method and its key features.

2.1 General principle of CCI

The CCI methods are based on the cross-coherence analysis of two low-coherence light beams, the object beam being reflected from the object t, whilst the reference beams is reflected from a reference mirror. The general idea of this method is shown in Figure 1. The high-contrast interference pattern arises if the optical path length in the object arm is equal to the optical path length in the reference arm. For each object point a correlogram is recorded during the movement of the object. The position of the corresponding object point along the x-axis can be measured by another measuring system for the maximum of the correlogram (step B in Figure 1). An interference signal is helpful for accurate determining of this position.
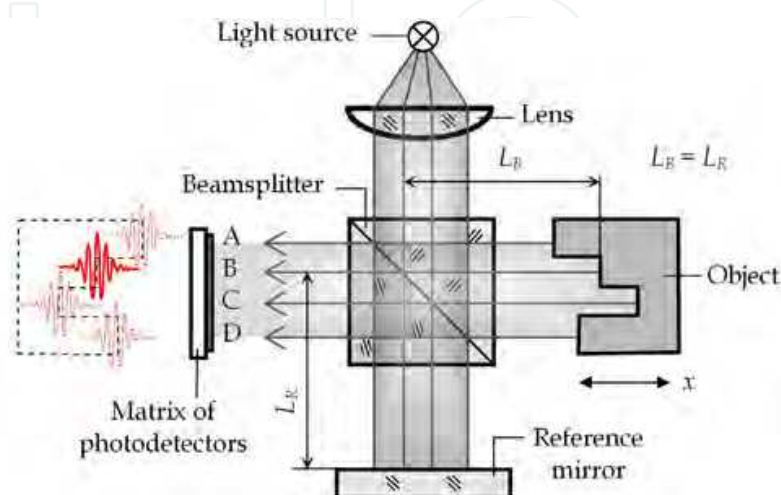

Fig. 1. Principle of the coherence correlation interferometry.

In the methods based on an assessment of the degree of temporal coherence of two interfering beams white light or low coherence light is used. These methods are incorporated in many types of measuring instrument. One of the most commonly used is the white-light interference microscope. This instrument combines the three most important features: white- light illumination, interference objective lenses and a precision scanner. The principle of operation applied in many white-light interference microscopes is based on the CCI technique.

2.2 Features of CCI

Features of CCI include:

* wide measuring range and high resolution,
* a large measurement area on the object,
* short time of measurement,
* exceptional versatility for for measuring objects made from different materials.

Similarly, the modern white-light interference microscopes have a number of advantages, e.g. wide measuring range, high accuracy and short time of measurement. The range of applications of white-light interference microscopes is very wide and includes:

* material sciences and engineering (analysis of structures of the polymer materials),
* mechanics (measurement of surface topography of the precision machined parts and elements, measurements of the smooth and super-smooth surfaces),
* electronics (measurements of silicon wafers),
* analysis of the surface structures of micro electro-mechanical systems (MEMS) and micro-opto-electro-mechanical systems (MOEMS),
* optics (measurements of optical elements e.g. microlenses, diffractive optics).

3. Theory

The third section will focus on theoretical basis of coherence correlation interferometry. This section will also cover a discussion of partially coherent wave interference and an analysis of a dependence upon the complex degree of coherence in interfering waves from a surface topography.

3.1 Coherence of light

The temporal coherence of light is connected with the phase correlation of the light waves at a given point in space at two different instants of time. It is characterized by coherence length, i.e. the propagation distance over which coherence of the beam is kept. Temporal coherence is a measure of the correlation between the phases of a light wave at different points along the direction of propagation. When we deal with two light waves then mutual temporal coherence can be analysed. This is a measure of the cross-correlation between the phases of these waves.

In coherence theory a complex degree of coherence is a measure of the coherence between two waves. This measure is equal to the cross-correlation function between the normalized amplitude of one wave and the complex conjugate of the normalized amplitude of the other:

$$\gamma_{12}(\tau) = \frac{\Gamma_{12}(\tau)}{\left[\Gamma_{11}(0)\Gamma_{22}(0)\right]^{1/2}} \, , \qquad (1)$$

where: $\gamma_{12}(\tau)$ – complex degree of mutual coherence, τ – time delay, $\Gamma_{12}(\tau)$ – function of mutual coherence of light, $\Gamma_{11}(0)$, $\Gamma_{22}(0)$ – self-coherence functions of light.

3.2 Use of CCI for surface topography measurements

Typically a two -beam interferometer (e.g. Michelson's, Linnik's or Mirau's interferometer) is used in coherence correlation interferometry. The two -beam interferometer is illuminated by a light source with a low degree of temporal coherence light. The optical path length in one arm of the interferometer changes during measuring and the interference signal is then analysed.Advanced analysis of the signal is carried out on every single point of the evaluated surface. In most cases this consists in determining the interference signal's envelope maximum. The shape of the interference signal depends on the complex degree of cross-coherence of the interfering waves.

Let the two partially coherent light waves with an average frequency v_0 and equal intensities I_0 interfere in the system interference microscope. One of the waves reflected from the surface of the test with $z(x, y)$, and the other from the reference mirror. The light intensity I in the selected point interference field is determined by the equation:

$$I = 2I_0\left[1 + \left|\gamma_{12}(\tau)\right|\cos\alpha_{12}(\tau)\right] \, , \qquad (2)$$

where: I_0 – intensity of interfering waves, α_{12} – function, which defines phase difference of interfering waves.

As shown in equation (2) an interference signal depends on the complex degree of mutual coherence γ_{12} in interfering waves. The complex degree of mutual coherence γ_{12} can be interpreted as a normalized cross-correlation function of the light wave reflected from the analysed surface and the wave reflected from the reference mirror.

$$\gamma_{12}(\tau) = \left|\gamma_{12}(\tau)\right|\exp\left\{-i\left[2\pi v_0\tau - \alpha_{12}(\tau)\right]\right\} \, , \qquad (3)$$

where: i – imaginary unit, v_0 – average frequency of interfering waves.

The complex degree of mutual coherence γ_{12} is analyzed separately at each point of the surface. If a test surface $z = f(x, y)$ is rough, it can be assumed that the complex degree of mutual coherence is a function depending not only on the parameter τ, but also on the coordinates x and y. Time delay τ is zero at the considered point of the surface for such position z_0 of scanning system at which the lengths of optical paths in both arms of the interferometer are equal. The parameter value of τ for the position of z is determined from the relation:

$$\tau = \frac{2(z-z_0)}{c}, \qquad (4)$$

where: z – position of the scanning system of interferometer, z_0 – position of the scanning system at which the lengths of optical paths in both arms of the interferometer are equal, c –speed of light.

Measurement of surface topography using the CCI is based on analyzing the time delay values $\tau (x, y)$ between the interfering waves at different points of the surface. Time delay is function x and y which is changing during the scanning process. It is possible for each point of the surface to determine the position of $z = z_0$, for which $\tau = 0$. As a result, such a measurement is obtained through discrete function $z = z_0(x, y)$ that describes a set of points. Each point is defined by three coordinates x, y, z. This imaging of the shape of the surface possible.

Fig. 2 shows a graph of relative light intensity at some point of the interference image depending on the position of the scanning system. The physical quantity λ_0 shown in Figure 1 is the average wavelength of light and can be determined from the relationship:

$$\lambda_0 = \frac{c}{v_0}. \tag{5}$$

The graph shown in Figure 2, in fact, describes the cross-correlation function of the interfering waves and the envelope of this function.
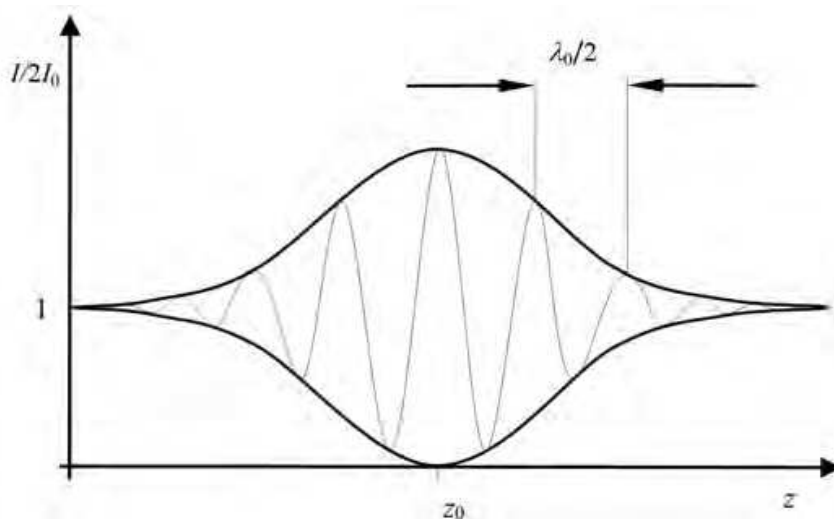

Fig. 2. Relative light intensity at some point of the interference image

4. Implementation of the CCI for surface topography measurements

Issues related to the implementation of CCI in instruments for surface topography assessments are presented in this section. The construction and general metrological characteristics of some of them (e.g. Taylor Hobson, Veeco and Zygo) are given. This section will also consist of a description of the three main interference objective lenses (Michelson, Mirau and Linnik) used in CCI instruments, as well as relevant diagrams and technical specifications characterizing these objective lenses. In the final part of the section, selected algorithms used in the practical implementation of surface topography measurements, using CCI, are discussed.

4.1 Construction of typical CCI instruments

Typical CCI instruments are equipped with the measurement base supported on an antivibration table. The antivibration table is used for separating the instrument from external vibration sources. Usually the granite slab can fulfill the role of the anti-vibration table. In other instances more advanced solutions are used, such as active vibration isolation systems. The translating table and a vertical column are mounted upon the measurement base. The translating table enables tilt adjustment (by several degrees) around x and y axes (in some instruments also with z axis rotation). Tilt adjustment is one of the pre-measurement procedures. This procedure is especially useful for samples, which are characterized by high angles of slope and high values of surface irregularity. Movement and adjustment of the stage can be realized manually or motorized by joystick control. The main elements of a typical CCI instrument (Talysurf CCI 6000 produced by Taylor Hobson Ltd., (UK)) are shown in Fig. 3.
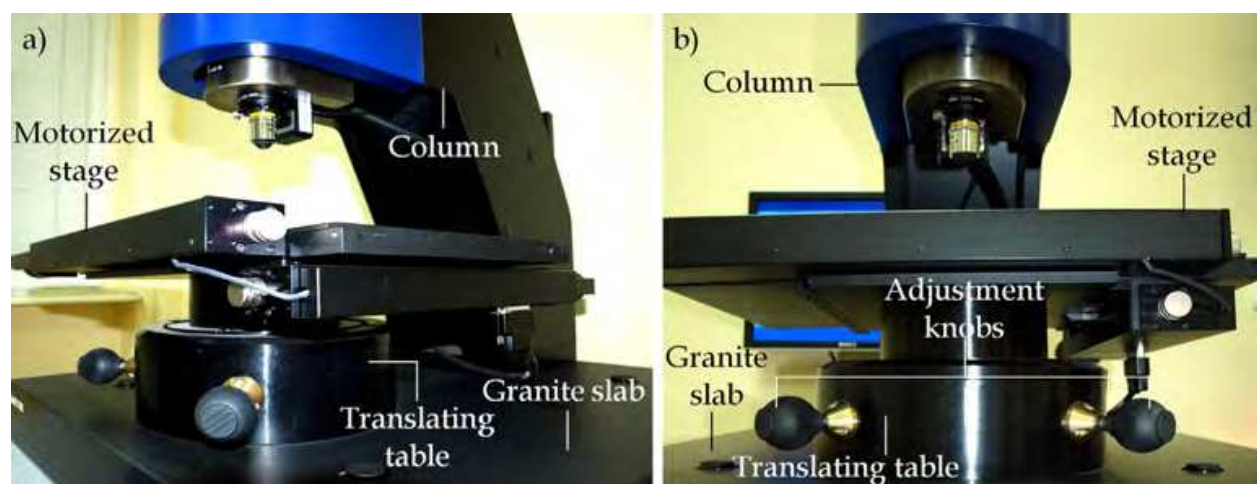

Fig. 3. White-light interference microscope Talysurf CCI 6000 produced by Taylor Hobson Ltd., (UK): a), b) front view and side view of the instrument with the main elements.

The optical interferometry and vertical scanning systems are located in a column. A source of light can be installed in compact form in the optical interferometry system or can be located outside the instrument. In this case a specially designed illuminatore was usually utilised. Light from the illuminator to the interferometer's optical system is delivered by an optical fibre.

An integral part of the CCI instrument is a stationary computer and a one or more computer monitors. Computer must be characterized by a high speed computing and adequate HDD free storage space for the archiving of recorded measurement data. In addition to controlling the CCI instrument and recording measurement data, the computer is used for processing and analysis of data. This process is realized by the use of specialist software, which is usually supplied by the producer of the CCI instrument.

4.2 General characteristics of the CCI instruments

The CCI instruments are characterized by certain metrological parameters (Leach et al., 2008; Petzing et al., 2010), which are specified in the technical specifications. Metrological

parameters are a necessary source of information for determining the requirements for the purchase and later operation of instruments. A description of the selected metrological parameters is given below.

- Vertical resolution (*z* axis) is the ability of the CCI instrument to resolve a surface profile vertically (in z axis). Vertical resolution for commercial instruments is in the range from 0.01 nm to 0.5 nm.
- Lateral resolution (*x* and *y* axis) is defined as one-half the spatial period for which the instrument response (measured height map compared to the actual surface topography map) falls to 50 %. Lateral resolution for commercial instruments depends on the magnification and can be between 0.5 µm to 7 µm.
- Repeatability is the ability of an instrument to provide similar indications for repeated evaluation of the same measurement under the same conditions of measurement. Repeatability for commercial instruments is between 0.002 nm to 50 nm. For example: for the white-ligt interference microscope TMS-1200 TopMap µ.Lab produced by Polytec (Germany) repeatability (at 10 nm sampling increment) is 0.25 nm (smooth surface) as well 2.5 nm (rough surface) and (at 87 nm sampling increment) is 0.5 nm (smooth surface) and 20 nm (rough surface).
- Instrument noise is typically a small random error term superimposed on the measurement data. The source of this noise can be electronic components and devices mounted on the instrument (e.g. amplifiers, stabilizers, detectors). Some manufacturers provide software procedures, which neutralise this effect.

Selected metrological parameters, which characterize some of the commercially interferential microscopes available on the market are presented in Tab. 1. Similar metrological parameters for selected four instruments of the Talysurf CCI line manufactured by Taylor Hobson Ltd., are presented in Tab. 2.

Instrument	Producer	Method	Vertical range (mm)	Vertical resolution (nm)	Measurement area (max.) (mm)
MarSurf WS1	Mahr	SWLI	0.1	0.1	1.6 × 1.2
TMS-300-214 TopMap In.Line	Polytec	SWLI	0.5	<0.55	18.6 × 13.9
Wyko NT1100	Vecco	PSI/VSI	1	0.01	8.24 × 8.24
WLI	MRC	VSI	0.15	1	0.25 × 0.25

Table 1. Selected metrological parameters of commercially available interferential microscopes.

The CCI instruments are a large group of advanced optical measurement systems currently used in many fields of modern science and technology. There are a number of commercial CCI instruments available on the market. They are produced by Fogale, Mahr, MRC, Phase Shift, Polytec, Taylor Hobson Ltd., Vecco, and Zygo. Some examples of commercially available white-light interference microscopes are shown in Fig. 4.

Instrument	Method	Vertical range* (mm)	Vertical resolution (nm)	Repeatability of surface (nm)	Measurement area** (mm²)
Talysurf CCI Lite	CCI	2.2	0.01	0.002	6.6
Talysurf CCI 9150	CCI	0.1	0.01	0.003	0.25 - 7.0
Talysurf CCI 6000	CCI	0.1	0.01	0.003	0.36 – 7.0
Talysurf CCI 3000	CCI	0.1	0.01	0.003	0.36 – 7.2

*Standard range (optional, can be extended), **Square area

Table 2. Selected metrological parameters for instruments of the CCI line manufactured by Taylor Hobson Ltd., (UK)

Fig. 4. The commercially available white-light interference microscopes: a) Wyko NT1100 produced by Veeco (Vecco Instruments, 2002), b) NewView™ 7300 produced by Zygo (Zygo Corporation, 2010), c) NewView™ 600 produced by Zygo (Zygo Corporation, 2007)

4.3 Interference objective lenses

Modern interference microscopes typically use standard microscope objective lenses, containing one of three types of classic two-beam interferometer, the configuration of which has been appropriately modified to enable the measurement of such instruments:

- Linnik interferometer (Linnik, 1933),
- Mirau interferometer (Delaunay, 1953; Kino & Chim, 1990),
- Michelson interferometer (Michelson, 1882).

The last two of these interferometers are most commonly used in CCI instruments. In a Mirau interferometer the basic elements are a microscope objective lens, a reference surface and a beamsplitter. All the elements are on the same optical axis of the objective lens. In this configuration, there are two paths from the light source to the detector. In the first path a light beam reflects off the beamsplitter, passes to the reference mirror and then reflects back, before passing through the beamsplitter to the microscope objective lens and then on to the detector. In the second path, a light beam passes through the beamsplitter, to the reference mirror, reflects back to the beamsplitter and then reflects from the half mirror into the microscope objective lens before proceeding to the detector. The light reflected from these surfaces recombines and a fringe interference pattern is formed. The objective lenses with Mirau interferometer are usually used in applications requiring higher magnification (>10×) or numerical apertures. In such instances objective lenses can be used following typical 10×, 20×, 50× and 100× magnification.

A Michelson interferometer is configured in a similar way to a Mirau with the exception that the reference mirror is in a different position (outside the optical axis). This configuration provides a longer working distance, wider fields of view and larger depth of focus at small magnifications (<5×). The following magnification can be typically used for objective lenses with a Michelson interferometer: 1×, 1.5×, 2×, 2.5× and 5×.

Commercial microscope objective lenses with interferometers are manufactured by Leica, Nikon, Olympus, Seiwa Optical, Veeco, Zeiss and Zygo. Availability of wide range of interference objective lenses give a great opportunities concerned with selection of the suitable lens for carrying out scientific works. Selected issues related with suitable selection of interference objective lenses were described in the work (Petzing et al., 2010). Schematic diagrams of the typical configurations of interference objective lenses are shown in Fig. 5, whereas the general characteristics of interference objective lenses produced by Nikon (Japan) are presented in Tab. 3.
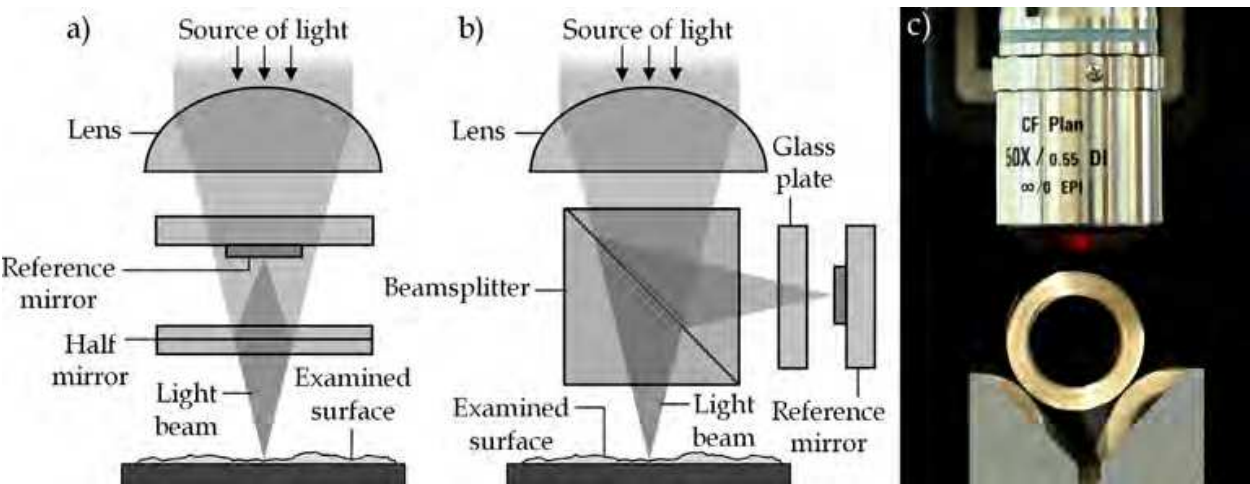

Fig. 5. Schematic diagrams of the typical configurations of interference objective lenses: a) Mirau, b) Michelson, c) commercially produced microscope objective lens with Mirau interferometer (Nikon 50× CF Plan IC EPI).

Designation of objective lens	Magnification	Numerical aperture	Working distance (mm)	Focal lenght (mm)	Weight (g)
2.5× CF Plan IC EPI	2.5×	0.075	10.3	80	440
5× CF Plan IC EPI	5×	0.13	9.3	40	280
10× CF Plan IC EPI	10×	0.3	7.4	20	125
20× CF Plan IC EPI	20×	0.4	4.7	10	130
50× CF Plan IC EPI	50×	0.55	3.4	4	150
100× CF Plan IC EPI	100×	0.7	2	2	200

CF – Chrome-Free, Plan – Flat Field Correction, IC – Infinity Corrected, EPI – Epi Illumination

Table 3. General characteristics of interference objective lenses produced by Nikon (Japan)

4.4 Algorithms

The accuracy of surface topography measurements using the CCI is dependent on many factors. One of the most important factors is the algorithms used during the scan and the interference signal analysis algorithms. Analysis of signal interference generally requires the use of algorithms determining the maximum envelope of the signal (CCI mode) an the phase image-based interference (PSI mode).

An algorithm for digital envelope detection in white-light interferograms was described in the work (Larkin, 1996). It was compared with other algorithms. It was developed based on algorithms used in the PSI methods (Creath, 1988; Stahl, 1990; Kujawinska, 1993). The new algorithm was assessed in terms of accuracy and computational efficiency. It can be interpreted as a second-order nonlinear filter. Use of quadrature modulation and Hilbert transformation as a new measurement strategy, based on a direct reconstruction of the envelope of the correlogram, was presented in the paper (Hybel et al., 2008).

At work (Park & Kim, 2000) proposed the use of a new algorithm for detecting the true peak of the interference fringe. This two-step algorithm is an efficient means of computation to obtain a good measuring accuracy with greater insulation against disturbances and noise.

In order to obtain high accuracy and performance out of CCI and PSI techniques, many algorithms have been proposed (Ailing et al., 2008; Buchta et al., 2011; Kim et al., 2008). Among those algorithms analyzed were: phase-shifting, phase-crossing (Pawłowski et al., 2006), zero-crossing and Fourier-transform techniques. Algorithms that give an estimate of the envelope peak position from only a fraction of the interferogram (Sato & Ando, 2009) were also proposed.

Within the CCI techniques there were developments in scanning algorithms, merge and stitch images and error correction (Viotti et al., 2008; Kim et al., 2008), many of which have been patented and used in commercial systems (Harasaki & Schmit, 2002; Bankhead & McDonnell, 2009).

5. Measurements of engineering surfaces

The section is dedicated to some selected issues related to the applictaion of CCI for precise surface topography measurements (Conroy, 2008). A brief description of the white-light interference microscope Talysurf CCI 6000 by Taylor-Hobson Ltd., is presented. Subsequently issues related to the pre-measurements and measurements procedure, as well as processing and analysis of measurement data, are described in detail. The selected results of measurements of surface topography obtained by CCI for objects machined by various techniques are presented and discussed in the final part of this section.

5.1 Interference microscope with Mirau objective lenses

One of the commercially available CCI instruments is a white light interference microscope produced by Taylor Hobson Ltd. The firm produces this line of instruments under the designation Talysurf CCI. One of these instruments is Talysurf CCI6000 (Conroy & Armstrong, 2005; Cincio et al., 2008; Lukianowicz, 2010). The principle of operation of this instrument, shown in Fig. 6, is based on coherence correlation interferometry.

White light generated by an external source (150 W quartz lamp installed in Fiber-Lite® DC-950 illuminator manufactured by Dolan-Jenner's Industries) is supplied to the instrument by optical fibre. In the measuring head the light beam is directed to a beamsplitter, where it is separated into two parallel beams. The first beam is directed towards the sample and the second beam is directed towards an internal reference mirror. The two beams recombine and give a local interference image, which is sent to the CCD detector.
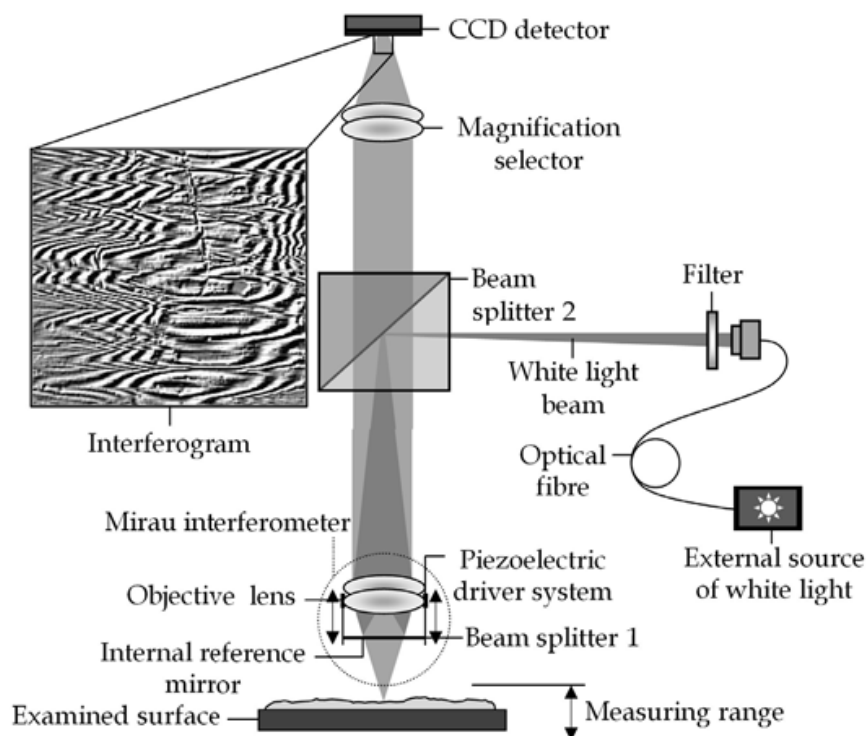

Fig. 6. Schematic diagram showing the principle of operation of the white-light interference microscope Talysurf CCI 6000 produced by Taylor Hobson Ltd.

The optical measuring head of the microscope is coupled with precision piezo-electric actuators (PZTs). The PZTs move the measuring head vertically above the measured sample.

The CCD detector measures the intensity of the light as the interferometric lens (Mirau type, 10×, 20× and 50× magnification) is actuated in the vertical direction (*z* axis) and finds the interference maximum. The location of individual points on the test surface is determined based on the analysis of the mutual temporal coherence of the interfering waves, conducted separately for each surface point.

In this way an image is generated and acquired, before being processed on a computer manufactured by Dell, with an Intel Xenon class processor. Using this recorded data a high-resolution surface topography is then generated. The instrument enables the obtainment of a vertical resolution to 10 pm (0.01 nm) at the measuring range (in the z axis) to 10 mm. Regardless of the magnification the surface topography contains more than one million data points (1024 × 1024 points).

The manufacturer of the instrument has supplied dedicated computer software. These are two applications: Talysurf CCI v. 2.0.7.3 (control elements of the system and measurements) and TalyMap Platinum v. 4.0.5.3985 (visualization and advanced data analysis). The TalyMap software uses Mountain Technology™ provided by DigitalSurf (France).

The general view of the white-light interference microscope Talysurf CCI 6000 produced by Taylor Hobson Ltd., is shown in Fig. 7.
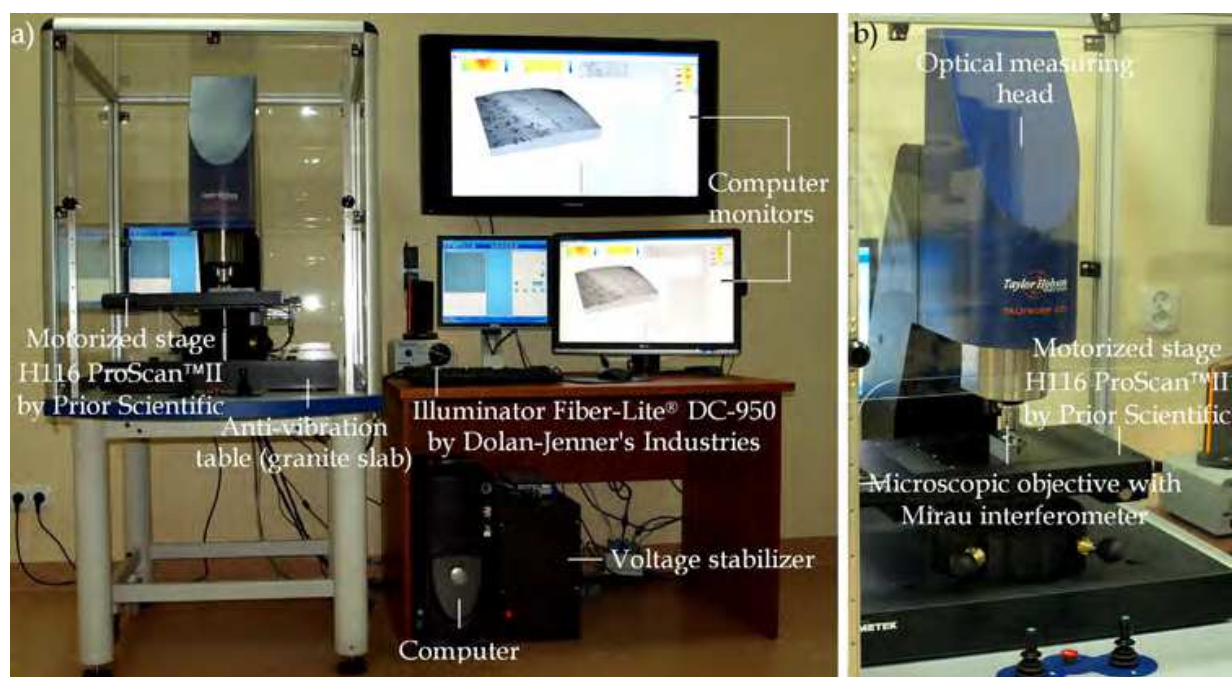

Fig. 7. White-light interference microscope Talysurf CCI 6000 produced by Taylor Hobson Ltd.: a) general view of the measuring system, b) near view of the instrument.

5.2 Pre-measurements procedure

The pre-measurements procedure for sample preparation usually involves:

- visual analysis of sample surface,
- cleaning the sample,
- overcoating of surface (optional, if necessary),
- fixturing the sample,
- orientation of sample.

The process requires a sample that must be clean and free from grease, smears, fingerprints, liquids and dust. If the samples are contaminated in some way before the measurement process begins they must be cleaned. Cleaning the sample would normally require the use of alcohol based liquids, or compressed air. Cleansing the sample surface is an extremely important issue, because the accumulated contamination can be generative source of measurement error.

In some cases, the reflective characteristics of a surface may hinder its measurement. This concern particularly affects those surfaces which are made of materials with relatively low reflectance. For such surfaces it may be desirable to overcoat with thin layers of vacuum coated gold or chromium.

The geometry and mass of the sample are the main factors affecting their method of fixturing. Use of non-permanent adhesives (e.g. adhesive tape, gels for fixturing etc.), may cause creep, whereas use of external force may cause sample distortion. Usually a range of table mounting points and accessories are used in the laboratory, including:

- magnetic and vacuum chucks/plates,
- disk fixtures
- tray holders.

The orientation of the sample may affect the results of the measurements. It is necessary to determine the proper orientation for all measured samples to obtain this same repeatability.

5.3 Measurements procedure

After the proper sample preparation the measuring procedure can begin. A typical measurement procedure (regardless of the CCI instrument) involves the following steps:

- power up the instrument and the computer,
- run the program (for control/measurements) on the computer,
- select the objective lens for the measurement,
- place the test element on the stage (adjusting the x and y axes),
- position the objective lens at its working distance from the element (adjusting the z axis),
- focus the microscope to obtain a sharp image,
- adjust stage level or tilt to optimize fringe contrast/appearance,
- adjust the test element position (x and y axes),
- minimize the number of fringes,
- adjust the light intensity level to an optimum value,
- check correct software-selectable items,
- initiate data acquisition.

A more detailed description of objective lens selection and image stitching procedures is presented below. Descriptions of other steps can be found also in (Leach et al., 2008; Petzing et al., 2010).

One of the important steps during the measuring process is selection of the objective lens. From a practical point of view it is most important to determine the main characteristics of the measured surface. It is on this basis that an appropriate objective lens is usually selected. General information concerning the selection of the objective lens is presented in Tab. 4, whereas general views of two types of microscope objective lenses with Mirau interferometer (used for surface roughness measurement) produced by Nikon (Japan) are show in Fig. 8.

Surface			Objective lens	
Area size	Surface element	Resolution	Magnification	Type of interference objective lens
Small	Steep slopes, rough surfaces	High	10×, 20×, 50×, 100×	Mirau
Large	Flat and smooth surfaces	Low	1×, 1.5×, 2×, 2.5×, 5×	Michelson
Very large			1×, 1.5×, 2×, 2.5×, 5× +image stitching procedure	

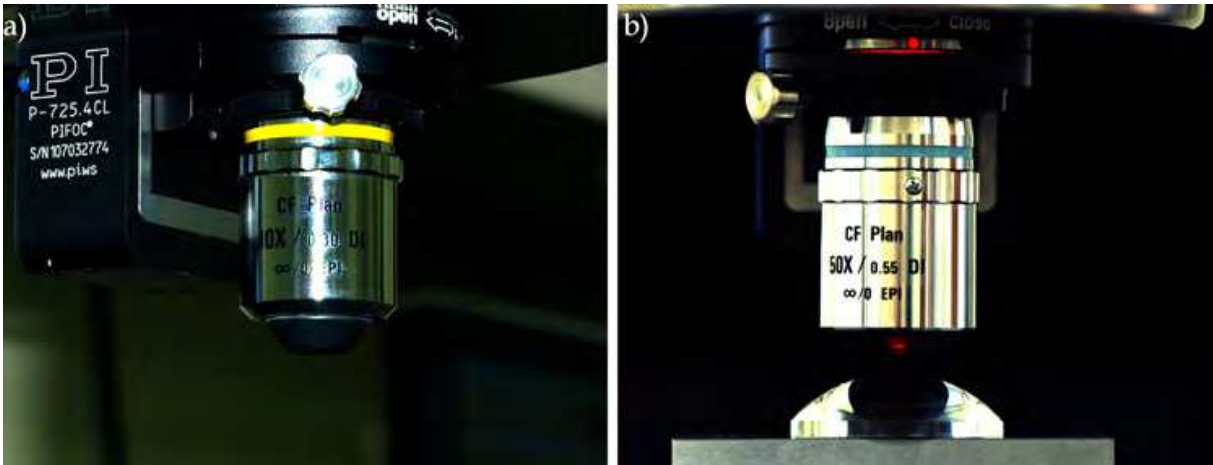Table 4. General information on selection of the objective lens.

Fig. 8. Two types of the microscope objective lenses with Mirau interferometer used for surface roughness measurement: a) Nikon 10× CF Plan IC EPI (field of view 1.8 × 1.8 mm), b) Nikon 50× CF Plan IC EPI (field of view 0.36 × 0.36 mm).

In some cases there is a need for measurement of a larger area than that which would constitute the field of view of the objective lens. This is when the image stitching procedure, whereby a matrix of mages are joined, or stitched, together, can be utilised. Image stitching can be realized only if the CCI instrument is fitted with a motorized stage with horizontal translation, which allows the computer program to precisely adjust the surface position. Each acquired image is precisely positioned and there is a consistent overlap of images. This is important because it allows for a comparison of neighbouring images, and enables the precise correlation of lateral position and consistent vertical range values. The typical overlap between images ranges from 0 % to 25 %.

The operations of the image stitching procedure are described below using the example of the functions implemented in TalyMap Platinum software. This function is realized by
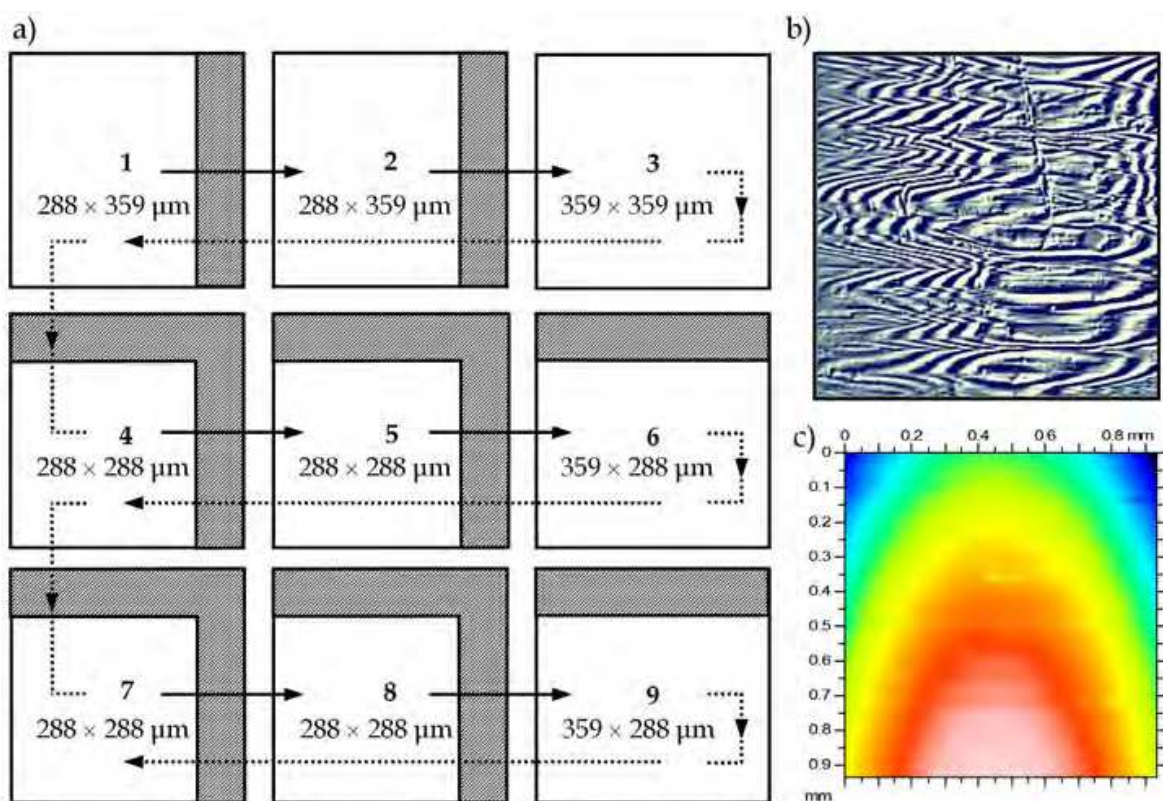
Fig. 9. The method of measurement of surface topographies with use of an image stitching function realized by TalyMap Platinum software: a) principle of image stitching procedure, b) single interferential image of measured surface with magnification 50×, c) output surface topography as a mosaic composed from a series of single surface topographies acquired as a 3 × 3 matrix.

Visual Basic script called Advances DataStiching v.1.2.1. In this case, the output surface topography is a mosaic composed of the 9 single surface topographies recorded as a 3 × 3 matrix.

A microscope objective lens with Mirau interferometer 50× CF Plan IC EPI, produced by Nikon, was used in the acquisition of the surface topographies The area measured for each of the topographies was the same 359 × 359 µm. During the stitching procedure, the area was often reduced by an overlap to a size 288 × 359 µm, 359 × 288 µm and 288 × 288 µm. The visual interpretations of the operations of the image stitching procedure are shown in Fig. 9.

5.4 Processing, analysis and interpretation of the results of measurements

Procedures relating to processing, analysis and interpretation (Petzing et al., 2010) are an important part of the measurement process following the acquisition of measurement data. In practice, these procedures are realized by special computer software. The popular commercial softwares for processing and analysis of measurement data include: Mountains Map by DigitalSurf (France), TrueMap by TrueGage (USA) and SPIP by Image Metrology A/S (Denmark). The pre-processing of measurement data usually includes (depending on software used):

- opening the file,
- levelling ,
- filling non-measured points.

After these procedures the file is ready to be processed, which will allow for the acquisition of:

- pseudo-colour surface maps,
- photo simulations,
- contour diagrams,
- mesh axonometrics,
- continuous axonometrics
- Abbot-Firestone curves,
- texture direction.

Above nly a few select procedures are given, in practice there may be many more.

They may also be more complicated and multi-threaded. Processing leads to the analysis, which typically involves:

- calculating the 2D parameters,
- calculating the 3D parameters.

As a result of analysis of the measurement data obtained, numerical values of the assessed paremeters characterizing the surface features are established.Based on these parameters and the machining parameters the whole machining process can be deduced. The interpretation of results in this case is very important, because it allows for the establishment of proper conditions within which the machining process will be optimally realised.

5.5 Examples of measurements and analysis

On the following pages some example results of analysis are shown, alongside collections of acquired surface topographies obtained by white-light interference microscope TalysurfCCI 6000 produced by Taylor Hobson Ltd., equipped with the TalyMap Platinum v.4.0.5.3985 software produced by DigitalSurf.

Fig. 10 presents an example analysis of a diffractive optical element (DOE) by Thorlabs, Inc. (USA).The DOEs are usually used in structured light generators. This sample has been manufactured from transparent polycarbonate. The value of light reflection coefficient for a polycarbonate surface was low, which made it a little awkward to analyse. The measurement was carried out on an area of approx. 4 sq. mm (Kaplonek & Tomkowski, 2009). Fig. 10 shows approx. 12% of the measured area (549 × 507 × 1.73 mm). The irregularities of this surface are periodical.

On Fig. 11 an example analysis of a 2.5″ HDD platter, by Toshiba Corp. (Japan), is shown.The topography has been measured on an area less than 1 sq. mm (980 × 979 × 0.06 μm). The irregularities of the surface are fairly insignificant and random. For these surfaces the values of 2D (*Ra,Rq, Rp, Rv, Rt, Rsk, Rku* and *Rz*) and 3D (*Sa, Sq, Sp, Sv, St, Ssk, Sku* and *Sz*) paremeters (Lukianowicz & Tomkowki, 2009) were also calculated. The collections of

Sample characteristics	Measuring instrument
Element: Diffractive optical element (DOE) Producer: Thorlabs, Inc. (USA) Material: polycarbonate	Instrument: Talysurf CCI 6000 Producer: Taylor Hobson Ltd., Software: TalyMap Platinum v. 4.0.5.3985
2D view: pseudo-colour surface map	**2D view: photo-simulation of surface**

2D view: surface profile and parameters	
	$Ra = 0.153$ μm $Rq = 0.205$ μm $Rp = 0.298$ μm $Rv = 0.562$ μm $Rt = 0.999$ μm $Rsk = -1.28$ $Rku = 4.18$ $Rz = 0.86$ μm

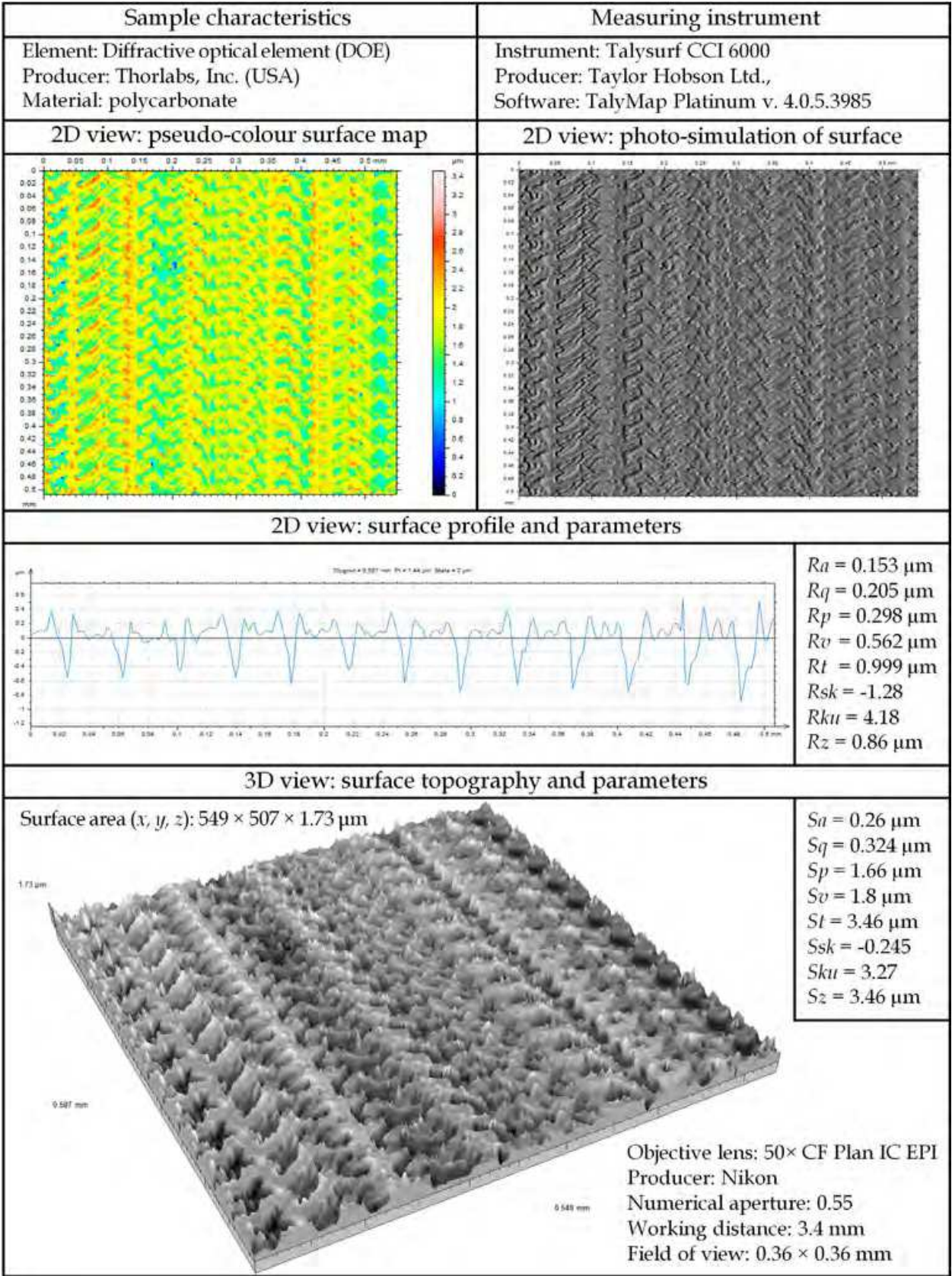| 3D view: surface topography and parameters	
Surface area (x, y, z): $549 \times 507 \times 1.73$ μm	$Sa = 0.26$ μm $Sq = 0.324$ μm $Sp = 1.66$ μm $Sv = 1.8$ μm $St = 3.46$ μm $Ssk = -0.245$ $Sku = 3.27$ $Sz = 3.46$ μm
	Objective lens: 50× CF Plan IC EPI Producer: Nikon Numerical aperture: 0.55 Working distance: 3.4 mm Field of view: 0.36 × 0.36 mm

Fig. 10. Exemplary analysis of a DOE sample for measurements obtained by white-light interference microscope Talysurf CCI 6000 produced by Taylor Hobson Ltd.
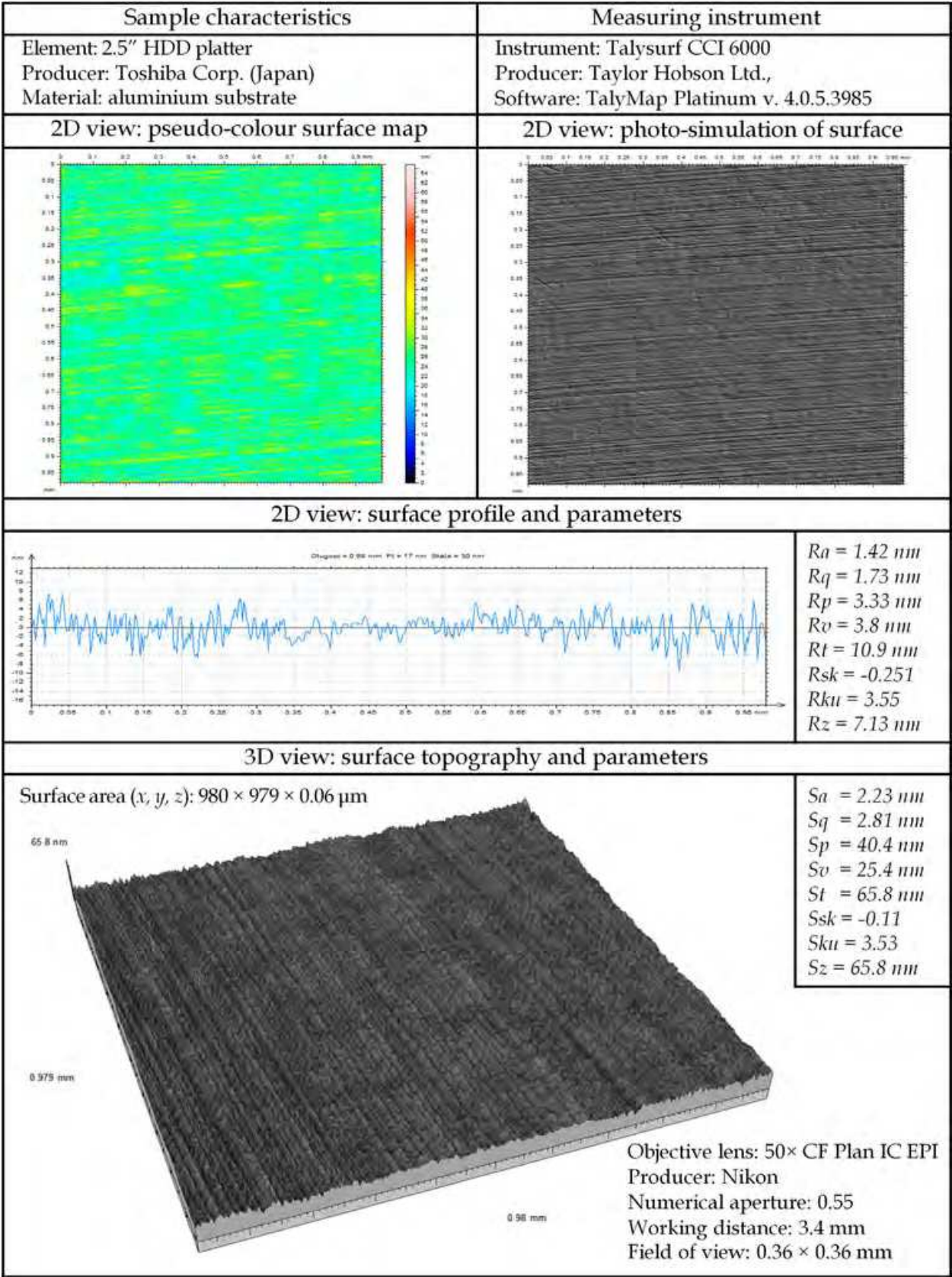
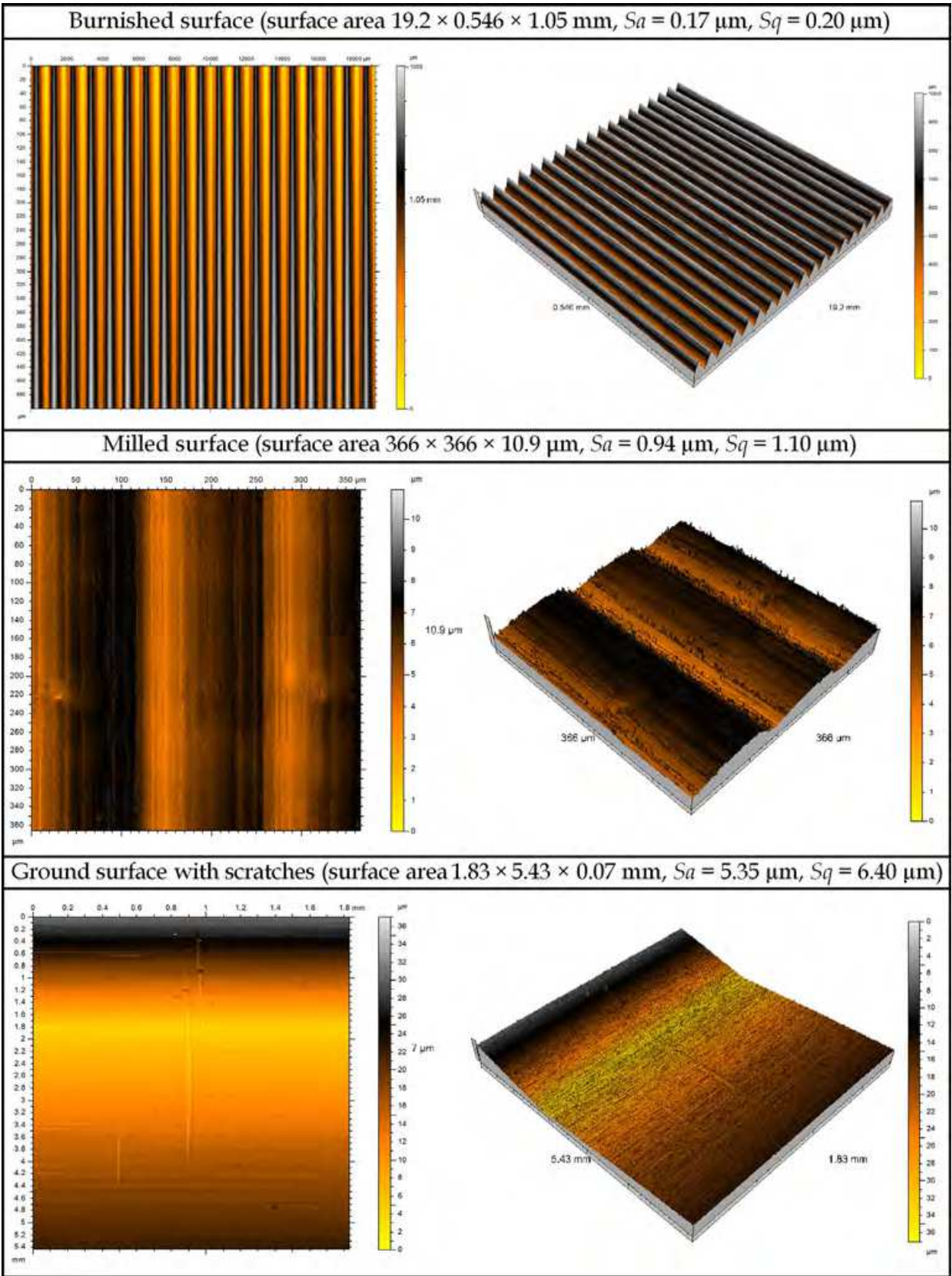| Sample characteristics	Measuring instrument
Element: 2.5″ HDD platter Producer: Toshiba Corp. (Japan) Material: aluminium substrate	Instrument: Talysurf CCI 6000 Producer: Taylor Hobson Ltd., Software: TalyMap Platinum v. 4.0.5.3985
2D view: pseudo-colour surface map	2D view: photo-simulation of surface

2D view: surface profile and parameters

$Ra = 1.42\ nm$
$Rq = 1.73\ nm$
$Rp = 3.33\ nm$
$Rv = 3.8\ nm$
$Rt = 10.9\ nm$
$Rsk = -0.251$
$Rku = 3.55$
$Rz = 7.13\ nm$

3D view: surface topography and parameters

Surface area (x, y, z): $980 \times 979 \times 0.06\ \mu m$

$Sa = 2.23\ nm$
$Sq = 2.81\ nm$
$Sp = 40.4\ nm$
$Sv = 25.4\ nm$
$St = 65.8\ nm$
$Ssk = -0.11$
$Sku = 3.53$
$Sz = 65.8\ nm$

Objective lens: 50× CF Plan IC EPI
Producer: Nikon
Numerical aperture: 0.55
Working distance: 3.4 mm
Field of view: 0.36 × 0.36 mm

Fig. 11. Exemplary analysis of a 2.5″ HDD platter sample for measurements obtained
by white-light interference microscope Talysurf CCI 6000 produced by Taylor Hobson Ltd.

Fig. 12. Collection of surface topographies obtained by white-light interference microscope Talysurf CCI 6000 produced by Taylor Hobson Ltd.

Fig. 13. Collection of surface topographies obtained by white-light interference microscope Talysurf CCI 6000 produced by Taylor Hobson Ltd.

topographies for different surfaces are shown in Fig. 12. and Fig. 13 (Kaplonek & Lukianowicz, 2010; Lukianowicz, 2010).

The first collection (Fig. 12) contains topographies of an engineering surface after the burnishing process. The value of the *x* axis is very high and amounts to 19.2 mm. This topography was generated using the image stitching procedure. In this same collection is a topography of a typically milled surface (measured area 366 × 366 × 10.9 μm) and a topography of a ground surface (measured area 1.83 × 5.43 × 0.07 mm) with defects in the form of scratches. These defects are typical for the surfaces of machine parts, which operate in industrial conditions.

In the second collection (Fig. 13) a polished surface is shown (measured area 0.359 × 0.359 × 7.9 μm) with a different defect, in this case taking the form of pitting. The next topography shows the surface of a grinding wheel 1-20×20×10 SG 80 M 8 V (measured area is 1.5 × 1.5 × 0.25 mm).

On the surface different sized abrasive grains are clearly visible. The last topography of this collection shows the surface of a calibration specimen, made for glass. Calibration specimens are usually used for routine calibrating of the stylus profilometers (measured area is 2.75 × 2.71 × 0.004 mm).

6. Limitations of CCI

During the interference measurements of surface topography some errors and limitations may be generated, for a number of different reasons. The sources of these errors are most often concerned with the measuring instrument and its software, as well as with the properties of the measured surface and the conditions in which the measurement was made. The limitations of CCI, and some factors affecting the accuracy of CCI based surface topography measurements, are discussed in this section.

6.1 Surface properties

One of the major contributing factors, which favor the generation of errors (Harasaki & Wyant, 2000, Pförtner & Schwider, 2001; Gao et al., 2008) in interference measurements of surface topography, are large gradients upon the surface analyzed. For such surfaces irregularities of slope and incline are significant.Slopes are usually described mathematically using the angles of slope tangent, surface derivatives or function gradient. In many cases, a considerable gradient causes the measurement errors due to limitations caused by the properties of the measuring instrument and its software. Fig. 14 shows three typical situations that may cause limitations in the measurement of surface topography:

- large slope angles of inequality,
- step height of surface irregularities,
- sloping recess.

No signal in the interference microscope caused by irregularities of slope occurs when, the slope angles of inequality θ exceed the maximum value θ_{max} given by the numerical aperture of the lens (Petzing et al., 2010):

$$\theta_{max} = \alpha_o = \arcsin\left(\frac{N_A}{n}\right), \qquad (6)$$

where: $N_A = n \sin\alpha_o$ – numerical aperture of interference microscope objective lens, n – refractive index of medium surrounding the objective lens, α_o – half the maximum value of the cone vertex angle formed by the rays from the microscope objective lens (Fig. 14a).
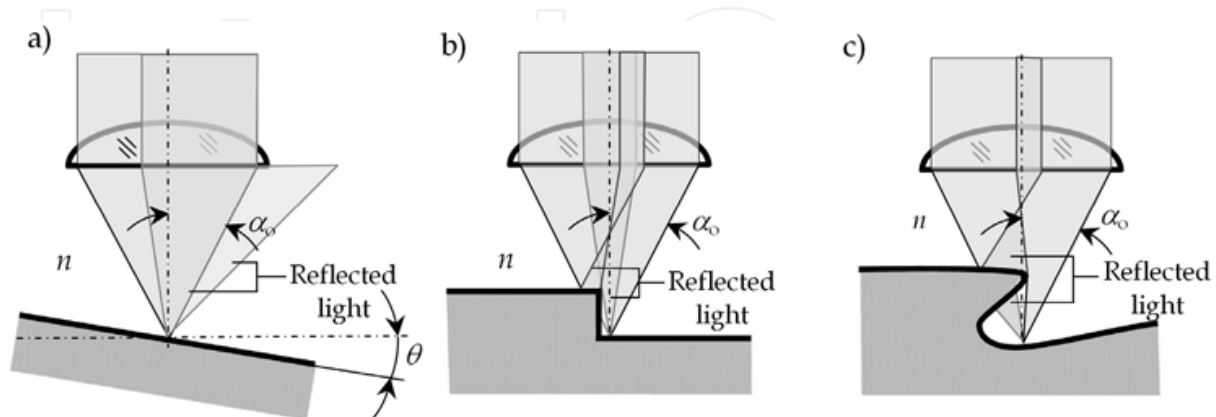

Fig. 14. Simplified diagram which showing the reflection of light focused by interference objective lens: a) from a sloped flat surface, b) from the surface with a step height, c) from the surface with sloping recess

Strong interference and no interference signal frequently reveal those surface areas, where there are significant step heights in surface irregularities or a sloping recess. During the measurements of these surfaces the self-shadowing of some areas, or partial self-shadowing of the light beam reflected from the surface, occurs (Fig. 14b and 14c).

For an analysis of the measurement errors of surface topography by interference methods, it is necessary to consider two models of surface irregularities. The first of these, is inequality, where the lateral dimensions are larger than the transverse resolving power d of an interference microscope objective lens given by the equation:

$$d = \frac{\lambda}{2N_A}, \qquad (7)$$

where: N_A – numerical aperture of interference microscope objective lens, λ – average wavelength of light used to illuminate the surface. The slopes of these inequalities can be regarded as smooth.

An interference image at a location corresponding to the slope will depend upon the shape of the surface. This image can be observed, if the slope angles do not exceed the specified maximum angle θ_{max} given by equation (6). However, if the slope angle of inequality as well as the slop of the surface are excessive, then the reflected radiation can be directed out of the microscope objective lens (Fig. 15a). In the second model, the transverse dimensions of irregularity are smaller than the transverse resolving power d of the interference microscope objective lens. Such surfaces can be considered as rough surfaces, which scatter the incidence light in a more or less diffuse way.In this case a part of the light scattered by the surface will be directed at the optical system of interfence microscope (Fig. 15b).

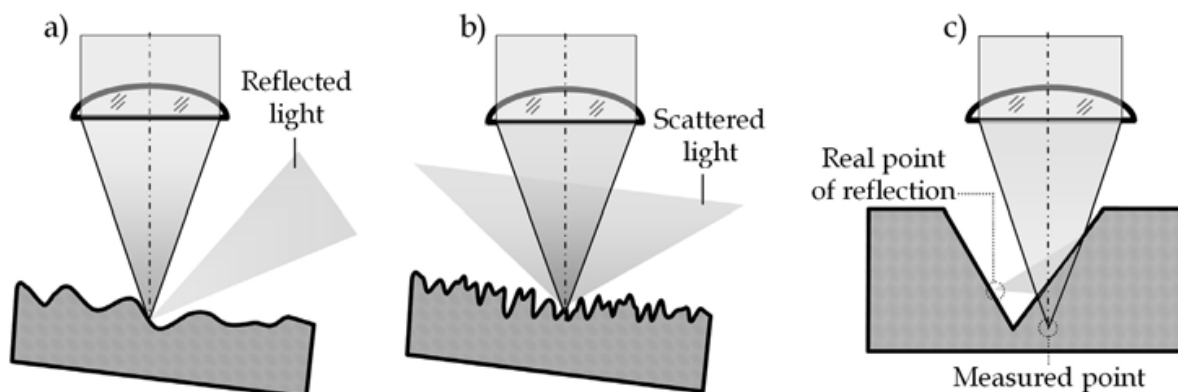Fig. 15. Double-reflection of light focused by interference objective lens on the surface of the measured wedge groove.

6.2 Instrumental and measuring environment limitations

The significant instrumental limitations of CCI are limited resolution of the lens aperture and the interference microscope objective lens, as well as the limitations concerned with the source of light and the scanning system.These limitations can cause inaccurate representation of the surface topography. The reason for the additional errors may be improper calibration of the measuring system, and imperfect software. Among the limitations related to the environment in which the measurement is carried vibrations and temperature changes are particularly noteworthy, as they cause random changes to occur in the measured surface topography. Limitations of CCI methods were discussed in more detail in (Petzing et al., 2010).

7. Conclusions

The results presented in this chapter show that coherence correlation interferometry is an advanced optical technique used for precise measurement of surface topography. The dynamic development of this technique means that it should play a dominant role in modern interference microscopy. CCI extends the scope of inferferometric techniques used in the measurement of surface topography. Especially those, which are characterized by complex structure or a relatively low reflectance (e.g. calibration specimens made from glass or transparent films).

The comparison between coherence correlation interferometry techniques and phase shifting methods shows that CCI has a better tolerance for variations in surface texture as well as greater capabilities for measuring surface features and structures, such as step heights. An important feature is also the fact that the point where the maximum interference occurs can be found for each single pixel of the detector. Additional advantages are concerned with large measurement ranges, high accuracy and repeatability as well as shortened times of measurement.
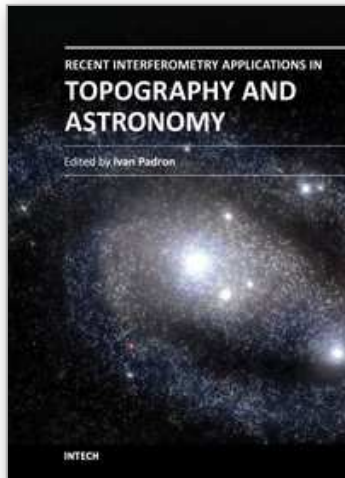
8. Acknowledgments

Engineering at Koszalin University of Technology, for measurements of engineering surfaces carried out by white-light interference microscope Talysurf CCI 6000.

9. References

Ailing, T.; Chunhui, W.; Zhuangde, J.; Hongjun, W. & Bingcai, L. (2008). Study on Key Algorithm for Scanning White-Light Interferometry, *Proceedings SPIE*, Vol. 7155, pp. 71552N-71552N, Ninth International Symposium on Laser Metrology, 30 June-2 July 2008, Singapore, ISBN 0819473987

Bankhead, A. D. & McDonnell I. (2008). Surface Profiling Apparatus, US Patent, No. 7385707 B2

Blunt, L. & Jiang, X. (Eds). (2003). *Advanced Techniques for Assessment Surface Topography*, Kogan Page Science, ISBN 1903996112, London, UK, Sterling, VA, USA

Blunt, R. T. (2006). White Light Interferometry – a Production Worthy Technique for Measuring Surface Roughness on Semiconductor Wafers, *Proceedings of CS MANTECH Conference*, pp. 59–62, Vancouver, British Columbia, Canada, April 2006

Buchta, Z.; Mikel, B.; Lazar, J. & Číp, O. (2011). White-Light Fringe Detection based on a Novel Light Source and Colour CCD Camera, *Measurement Science and Technology*, Vol. 22, 094031 (6 pp.), ISSN 0957-0233

Cincio, R.; Kacalak, W. & Lukianowicz, Cz. (2008). System Talysurf CCI 6000 – Methodic of Analysis Surface Feature with using TalyMap Platinium, *Measurement Automation and Monitoring*, Vol. 54, No. 4, pp. 187–191, ISSN 0032-4140 (in Polish)

Conroy, M. & Armstrong, J. (2005). A Comparison of Surface Metrology Techniques, *7th International Symposium on Measurement Technology and Intelligent Instruments*, Journal of Physics, Conference Series, Vol. 13, pp. 458–465, ISSN: 1742-6588, Huddersfield, UK, September 2005

Conroy, M. (2008). Advances in Thick and Thin Film Analysis using Interferometry, *Wear*, Vol. 266, Issue 5-6, pp. 502-506, ISSN 0043-1648

Creath, K. (1988). Phase-Measurement Interferometry Techniques, In: *Progress in Optics*, E. Wolf (Ed.), Vol. XXVI, pp. 349-393, North-Holland, ISBN 0444870962, Amsterdam, Netherlands

Creath, K. & Schmit, J. (2004). Phase Shifting Interferometry, In: *Encyclopedia of Modern Optics*, Guenther, R. D.; Steel, D. G. & Bayvel, L. (Eds), Vol. 2, pp. 364–74, Elsevier Academic Press, ISBN 0122276000, Amsterdam, Netherlands

de Grot, P. & Colonna de Lega, X. (2004). Signal Modeling for Low-Coherence Height-Scanning Interference Microscopy, *Applied Optics*, Vol. 43, No. 25, pp. 4821-4830, ISSN 0003-6935

Deck, L. & de Grot, P. (1994). High-Speed Noncontact Profiler Based on Scanning White-Light Interferometry, *Applied Optics*, Vol. 33, No. 31, pp. 7334-7338, ISSN 0003-6935

Delaunay, G. (1953). Microscope Interférentiel A. Mirau pour la Mesure du Fini des Surfaces. *Revue d'Optique Theorique et Instrumentale*, Vol. 32, pp. 610–614, ISSN 0035-2489

Gao, F.; Leach R.; Petzing J. & Coupland J. M. (2008). Surface Measurement Errors using Commercial Scanning White Light Interferometers, *Measurement Science and Technology*, Vol. 19, No. 1, pp. 015303 (13 pp.), ISSN 0957-0233

Harasaki, A. & Schmit, J. (2002). Bat-Wing Attenuation in White-Light Interferometry, United States Patent, No. US 6493093 B2

Harasaki, A.; Schmit, J. & Wyant J. C. (2000). Improved Vertical-Scanning Interferometry, *Applied Optics*, Vol. 39, No. 13, pp. 2107-2115, ISSN 0003-6935

Harasaki, A. & Wyant, J. C. (2000). Fringe Modulation Skewing Effect in White-Light Vertical Scanning Interferometry, *Applied Optics*, Vol. 39, No. 13, pp. 2101-2106, ISSN 0003-6935

Hariharan, P. (2007). *Basis of Interferometry* (2nd edition), Elsevier Academic Press, ISBN 9780123735898, Amsterdam, Netherlands

Hariharan, P. & Roy, M. (1995). White-Light Phase-Stepping Interferometry: Measurement of the Fractional Interference Order, *Journal of Modern Optics*, Vol. 42, pp. 2357–2360, ISSN 0950-0340

Hýbl, O.; Berger, A. & Häusler G. (2008). *Information Efficient White-Light Interferometry*, Deutschen Gesellschaft für angewandte Optik e.V. Proceedings, 109, A 29, Available from http://www.dgao-proceedings.de, ISSN: 1614-8436

Kaplonek, W. & Tomkowski, R. (2009). Analysis of the Surface Topography of Diffractive Optical Elements by White Light Interferometry, *Measurement Automation and Monitoring*, Vol. 55, No. 4, pp. 272–275, ISSN 0032-4140 (in Polish)

Kaplonek, W. & Lukianowicz, Cz. (2010). Use of Coherence Correlation Interferometry for Measurements of Surface Topography, *Electrical Review*, Vol. 86, No. 10, pp. 43–46, ISSN 0033-2097 (in Polish)

Kim, J.-H.; Yoon, S.-W.; Lee J.-H.; Ahn W.-J. & Pahk H.-J. (2008). New Algorithm of White-Light Phase Shifting Interferometry Pursing Higher Repeatability by using Numerical Phase Error Correction Schemes of Pre-Processor, Main Processor, and Post-Processor, *Optics and Lasers in Engineering*, Vol. 46, Issue 2, pp. 140-148, ISSN 0143-8166

Kino, G. S. & Chim, S. S. (1990). Mirau Correlation Microscope, *Applied Optics*, Vol. 29, No. 26, pp. 3775-3783, ISSN 0003-6935

Kujawinska, M. (1993). Spatial Phase Measurement Methods, In: *Interferogram Analysis: Digital Fringe Pattern Measurement Technique*, Robinson, D. W. & Reid, G. T. (Eds), pp. 141-193, IOP Publishing, ISBN 075030197X, Bristol and Philadelphia

Larkin, K. G. (1996). Efficient Nonlinear Algorithm for Envelope Detection in White Light Interferometry, *Journal of the Optical Society of America A*, Vol. 13, No. 4, pp. 832–843, ISSN 1084-7529

Leach, R.; Brown, L.; Jiang, X.; Blunt R.; Conroy, M. & Mauger D. (2008). Guide to the Measurement of Smooth Surface Topography using Coherence Scanning Interferometry, In: *NPL Good Practice Guide*, No. 108, n.d., Available from http://www.npl.co.uk

Leach, R. (Ed.). (2011). *Optical Measurement of Surface Topography*, Springer-Verlag, ISBN 9783642120114, Berlin, Heidelberg, Germany

Linnik, V. P. (1933). A Simple Interferometer for the Investigation of Optical Systems, *Doklady Akademii Nauk SSSR (Proceedings of the USSR Academy of Sciences)*, No. 1, pp. 208-210

Lukianowicz, Cz. (2010). Use of White Light Scanning Interferometry for Assessment of Surface Topography, *Measurement Automation and Monitoring*, Vol. 56, No. 9, pp. 1055-1058, ISSN 0032-4140 (in Polish)

Lukianowicz, Cz. & Tomkowki, R. (2009). Analysis of Topography of Engineering Surfaces by White Light Scanning Interferometry, *Proceedings of 12th International Conference on Metrology and Properties of Engineering*(Pawlus P.; Blunt L.; Rosen B.-G.; Thomas T.; Wieczorowski M. & Zahouani H. Eds.), pp. 63–67, Rzeszow, Poland, ISBN 978-83-7199-545-3

Michelson, A. A. (1882). Interference Phenomena in a New Form of Refractometer, *The American Journal of Science*, Vol. 23, No. 3, pp. 120-129, ISSN 0002-9599

Niehues, J.; Lehmann, P. & Bobey, K. (2007). Dual-Wavelength Vertical Scanning Low-Coherence Interferometric Microscope, *Applied Optics*, Vol. 46, No. 29, pp. 7141-7148, ISSN 0003-6935

Park, M.-C. & Kim, S.-W. (2000). Direct Quadratic Polynomial Fitting for Fringe Peak Detection of White Light Scanning Interferograms, *Optical Engineering*, Vol. 39, No. 4, pp. 952-959, ISSN 0091-3286

Patorski, K.; Kujawińska, M. & Sałbut, L. (2005). *Laser Interferometry with Automatic Fringe Pattern Analysis* (1st edition), Patorski, K. (Ed.). Oficyna Wydawnicza Politechniki Warszawskiej, ISBN 9788372074911, Warszawa, Poland, (in Polish)

Pawłowski, M. E.; Sakano, Y.; Miyamoto, Y. & Takeda, M. (2006). Phase-Crossing Algorithm for White-Light Fringes Analysis, *Optics Communications*, Vol. 260, Issue 1, pp. 68–72, ISSN 0030-4018

Petzing, J.; Coupland, J.; & Leach R. (2010). The Measurement of Rough Surface Topography using Coherence Scanning Interferometry, In: *NPL Good Practice Guide*, No. 116, n. d., Available from http://www.npl.co.uk

Pförtner, A. & Schwider, J. (2001). Dispersion Error in White-Light Linnik Interferometers, *Applied Optics*, Vol. 40, No. 34, pp. 6223-6228, ISSN 0003-6935

Pluta, M. (1993). *Advanced Light Microscopy, Vol. 3, Measuring Techniques*, North Holland, ISBN 9780444988195, Amsterdam, Netherlands

Sato, S. & Ando, S. (2009). Weighted Integral Method in White-Light Interferometry: Envelope Estimation from Fraction of Interferogram, *Proceedings SPIE*, Vol. 7389, pp. 73892V-8, Optical Measurement Systems for Industrial Inspection VI, 15-18 June 2009, Munich, Germany, ISBN 9780819476722

Schmit, J. (2005). White Light Interferometry, In: *Encyclopedia of Modern Optics*, Guenther, R. D.; Steel, D. G. & Bayvel, L. (Eds), Vol. 2, pp. 375–387, Elsevier Academic Press, ISBN 0122276000, Amsterdam, Netherlands

Stahl, H. P. (1990). Review of Phase-Measuring Interferometry, *Proceedings of the SPIE*, Vol. 1332, Optical Testing and Metrology III: Recent Advances in Industrial Optical Inspection, pp. 704-719, ISBN 9780819403933, San Diego, California, USA, July 1990

Thomas, T. R. (1999). *Rough Surfaces* (2nd edition), Imperial College Press, ISBN 0750300396, London, UK

Veeco Instruments Inc., (2002). *Wyko NT1100 Optical Profiling System*. (Brochure), Available from http://ppewww.physics.gla.ac.uk/~williamc/NT1100_spec.pdf

Viotti, M. R.; Albertazzi, A.; Dal Pont, A. & Fantin, A. V. (2007). Evaluation of a Novel Algorithm to Align and Stitch Adjacent Measurements of Long Inner Cylindrical Surfaces with White Light Interferometry, *Optics and Lasers in Engineering*, Vol. 45, Issue 8, pp. 852-859, ISSN 0143-8166

Whitehouse, D. J. (1994). *Handbook of Surface Metrology* (1st edition), Institute of Physics Publishing, ISBN 0750300396, Bristol and Philadelphia

Whitehouse, D. J. (2003). *Handbook of Surface and Nanometrology*, Institute of Physics Publishing, ISBN 0750305835, Bristol and Philadelphia

Wieczorowski, M. (2009). *Using Topographic Analysis in Measurements of Surface Irregularities*, Wydawnictwo Politechniki Poznańskiej, ISBN 9788371438066, Poznan, Poland, (in Polish)

Zygo Corporation, (2010). *NewView™ 7300 Specifications* (Brochure), Available from: http://www.zygo.com/met/profilers/newview7000/nv7300spec.pdf

Zygo Corporation, (2007). *NewView™ 600 3D Optical Profiler* (Brochure), Available from: http://www.zygo.com/met/profilers/newview7000/nv7300spec.pdf

Recent Interferometry Applications in Topography and Astronomy

Edited by Dr Ivan Padron

This book provides a current overview of the theoretical and experimental aspects of some interferometry techniques applied to Topography and Astronomy. The first two chapters comprise interferometry techniques used for precise measurement of surface topography in engineering applications; while chapters three through eight are dedicated to interferometry applications related to Earth's topography. The last chapter is an application of interferometry in Astronomy, directed specifically to detection of planets outside our solar system. Each chapter offers an opportunity to expand the knowledge about interferometry techniques and encourage researchers in development of new interferometry applications.

How to reference

In order to correctly reference this scholarly work, feel free to copy and paste the following:

Wojciech Kaplonek and Czeslaw Lukianowicz (2012). Coherence Correlation Interferometry in Surface Topography Measurements, Recent Interferometry Applications in Topography and Astronomy, Dr Ivan Padron (Ed.), ISBN: 978-953-51-0404-9, InTech, Available from: http://www.intechopen.com/books/recent-interferometry-applications-in-topography-and-astronomy/coherence-correlation-interferometry-in-surface-topography-measurements

INTECH
open science | open minds